Atmospheric Pollution Research 13 (2022) 101568

Contents lists available at ScienceDirect

Atmospheric Pollution Research

journal homepage: www.elsevier.com/locate/apr

Chemical characteristics and sources of $PM_{2.5}$ in the urban environment of Seoul, Korea

Seokwon Kang [a], Siyoung Choi [a], Jihee Ban [a], Kyunghoon Kim [a], Rahul Singh [a], Gyutae Park [b], Myeong-Bok Kim [a], Dong-Gil Yu [a], Joo-Ae Kim [c], Sang-Woo Kim [d], Moon-Soo Park [e], Cheol-Hee Kim [f], Meehye Lee [c], Gookyoung Heo [g], Yu-Woon Jang [h], Sang-Sub Ha [h], Taehyun Park [a,**], Taehyoung Lee [a,*]

[a] National Department of Environmental Science, Hankuk University of Foreign Studies, Yongin, 17035, Republic of Korea
[b] Air Pollution Engineering Division, Climate and Air Quality Research Department, National Institute of Environmental Research, Incheon, 22689, Republic of Korea
[c] Department of Earth and Environmental Sciences, Korea University, Seoul, 08826, Republic of Korea
[d] School of Earth and Environmental Sciences, Seoul National University, Seoul, 08826, Republic of Korea
[e] Department of Climate and Environment, Sejong University, Seoul, 05006, Republic of Korea
[f] Department of Atmospheric Sciences, Pusan National University, Busan, 46241, Republic of Korea
[g] National Air Emission Inventory and Research Center, Chungju, 28166, Republic of Korea
[h] Institute of Latin American Studies, Hankuk University of Foreign Studies, Yongin, 17035, Republic of Korea

ARTICLE INFO

Keywords:
Particle-into-liquid sampler
Seoul air quality
Aerosol
$PM_{2.5}$
Chemical characteristics

ABSTRACT

In Seoul, Korea, episodes of high concentrations of $PM_{2.5}$ (particulate matter ≤2.5 μm) continue to occur despite the enforcement of air quality standards. Seoul has several sources of pollution owing to its high population density. Therefore, this study evaluated the chemical characteristics of $PM_{2.5}$, including inorganic ions and various gases, focusing on those with concentrations exceeding the standard limit. The study was conducted from June 1 to August 22, 2018, in Seongbuk, and from March 29 to May 31, 2019, in Jungnang. Water-soluble inorganic ions of $PM_{2.5}$ were measured every 30 min using a particle-into-liquid sampler (PILS) combined with two ion chromatographs. In Seongbuk, ammonium sulfate was mainly caused by ammonium-poor conditions. In Jungnang, ammonium nitrate production occurred mainly due to ammonium-rich conditions. In both regions, during the occurrence of concentrations of $PM_{2.5}$ exceeding the standard limit, the proportion of nitrate among inorganic ions was the highest. In Jungnang, two emission sources located in the west and southwest were identified using a conditional probability function. Contaminants from the southwest had high concentrations of nitrates, presumably due to atmospheric stagnation and nitrate mixing in lower planetary boundary layer height due to an decrease in surface temperatures at dawn. Pollutants from the west had high concentrations of sulfates. These are generated through photochemical reactions from industrial complexes. Cluster analysis confirmed that 27.2% of the air was stagnant and flowed from the south. In most cases, air pollutants originated from western Korea and coastal China.

1. Introduction

Particulate matter <2.5 μm in aerodynamic diameter ($PM_{2.5}$) causes asthma and cardiovascular diseases when inhaled and has been reported to be associated with death from kidney and bladder cancers (McConnell et al., 2003; Pope III et al., 2006; He et al., 2017; Turner et al., 2017). It also decreases the Earth's surface temperature by reflecting solar radiation and absorbing particle moisture, thus producing fog, and reducing visibility (Charlson et al., 1992; Intergovernmental Panel on Climate Change, 2007; Wang et al., 2020). Because of these adverse effects, many countries have implemented policies to reduce $PM_{2.5}$. In addition, much research has been conducted on the formation of $PM_{2.5}$ and its

Peer review under responsibility of Turkish National Committee for Air Pollution Research and Control.
* Corresponding author.
** Corresponding author.
E-mail addresses: tpark@hufs.ac.kr (T. Park), thlee@hufs.ac.kr (T. Lee).

https://doi.org/10.1016/j.apr.2022.101568
Received 28 February 2022; Received in revised form 26 September 2022; Accepted 28 September 2022
Available online 1 October 2022

sources of pollution (Lang et al., 2017; Kang et al., 2020). For Korea, the average $PM_{2.5}$ standard was established in 2015 as 50 and 25 μg m^{-3} for the 24 h and annual periods, respectively. The standards were strengthened in March 2018 to 35 and 15 μg m^{-3} for the 24 h and annual averages, respectively, for the protection and regulation of $PM_{2.5}$ (Park et al., 2020a). However, despite these revised standards in Korea, $PM_{2.5}$ still occurs at high concentrations over 150 μg m^{-3}, and intense $PM_{2.5}$ episodes still occur in Seoul (Lee et al., 2022).

$PM_{2.5}$ is classified into two categories: primary $PM_{2.5}$, which is emitted directly from pollution sources, and secondary $PM_{2.5}$, which is generated through various chemical reactions of water-soluble inorganic ions (WSIIs) in the air (Lin et al., 2022; Zhang et al., 2022). $PM_{2.5}$ is composed of complex chemical components, such as organic and inorganic ions, black carbon, and crustal elements (i.e., Si, Al, Ca, and Fe). Among these species of components, WSIIs, especially sulfate (SO_4^{2-}), nitrate (NO_3^-), and ammonium (NH_4^+), which are collectively referred to as SNA, comprise the largest chemical components for 20–70% or even more than 70% of $PM_{2.5}$ (Tian et al., 2017; Guo et al., 2020; Jo et al., 2020; Do et al., 2021). SNA has been detected in ammonium nitrate (NH_4NO_3), ammonium sulfate ($(NH_4)_2SO_4$), and ammonium chloride (NH_4Cl), which are formed by the neutralization of acidic gases such as ammonia (NH_3), nitric acid (HNO_3), and sulfuric acid (H_2SO_4) (Jo et al., 2020; Do et al., 2021). WSIIs have been found to play an important role in the formation of haze caused by the intense scattering effect of $PM_{2.5}$ and can affect the size, composition, number density, hygroscopy, and acidity of $PM_{2.5}$ (Chen et al., 2021; Cheng et al., 2021; Ting et al., 2022). Additionally, WSIIs can degrade visibility and accelerate the formation of $PM_{2.5}$ (Begam et al., 2017; Tian et al., 2017; Guo et al., 2020; Cheng et al., 2021).

As of 2019, approximately 20% of the Korean population lived in Seoul, with around 50% of that residing in the Seoul metropolitan area (SMA) (Won et al., 2021). Owing to this high population density, various emission sources are in the SMA, such as construction, gas stations, and automobiles. In addition, many sources of various forms contribute to the highly polluted atmosphere in the SMA (Park et al., 2020b). Some studies have reported that secondary inorganic aerosols (SIA), such as sulfate and nitrate, constitute a large source of $PM_{2.5}$, in the SMA (Ryou et al., 2018; Park et al., 2020a, 2022). The SIA in the SMA were also affected by long-range transport from China and by emissions from around the SMA (Kim et al., 2021b, 2022). Therefore, it is necessary to understand the inflow and characteristics of the SIA in Seoul.

Previous studies have measured the SIA using filter sampling in ambient air (Zhang et al., 2019a, 2019b; Guo et al., 2020; Zhao et al., 2022). This method was used to collect particles in the ambient air on filters using a vacuum pump. The SIA on collected filters were extracted from deionized water or solvents and analyzed by ion chromatography. However, this filter sampling method may be affected by chemical and physical factors during the collection, storage, and extraction of the filters. Furthermore, it has a long processing time in the laboratory (a few hours to a few days) and produces low-resolution data, making it difficult to measure daily patterns or chemical reactions in ambient air (Tutsak and Koçak, 2019; Zhang et al., 2019a). To understand and identify the chemical composition and characteristics of $PM_{2.5}$, a particle-into-liquid sampler (PILS) combined with ion chromatography was used in this study during the summers of 2018 and 2019. In addition, this study identified major air pollution sources that could be targeted in future mitigation measures for $PM_{2.5}$.

2. Methods

2.1. Sampling sites

The physical and chemical properties of secondary PM precursors and PM in Seoul were measured from June 1 to August 22, 2018 (summer) in Seongbuk (37.585949 °N and 127.025420 °E) and from March 29 to May 31, 2019 (spring) in Jungnang (37.589729 °N and 127.079042 °E). The sampling sites were located approximately 5 km apart, both approximately 5 km northeast of Myeong-dong (downtown) in Jung-gu, Seoul. The Naebu Expressway is located approximately 1 km east of the Seongbuk sampling site, around which residential complexes are distributed. The Jungnangcheon and Dongbu Expressways are located approximately 700 m west of the Jungnang sampling site and are surrounded by nearby residential complexes (Fig. 1). In Table 3, note that $PM_{2.5}$ was not measured in 2018; instead, data from Yongdoo Elementary School (37.575698 °N, 127.028709 °E), located 1 km south of Seongbuk, were used.

2.2. Measurement equipment

2.2.1. Particulate matter measurement

To observe inorganic ionic components, such as SNA in secondary PM in central Seoul, a PILS (Metrohm, Switzerland) and ion chromatography (IC; 883 Basic IC Plus, Metrohm, Switzerland) were combined (PILS–IC) for sampling and measurement (Table 1). The PILS-IC was installed according to the method described by Kang et al. (2020). The PILS uses high-temperature (150 °C) water vapor to grow particles with a diameter larger than 50 nm and then collects the particles (Weber et al., 2001). The inlet flow rate of the PILS was approximately 16.7 L min^{-1}, which was adjusted by installing a pressure regulator at the rear end of the orifice. The particle size of the inserted samples was increased by the water vapor supplied by the steamer inside the PILS. The grown particles collided with the impactor plate and spread along its surface to a metal mesh located on the side of the impactor. The samples were mixed with Lithium bromide (LiBr), which was the internal standard; thus, the concentration was calculated by considering the dilution factor. The solution collected in the vial was automatically injected into the IC every 30 min using a syringe pump. For quality assurance/quality control (QC/QA) of inorganic ionic components, blank and standard solutions were measured periodically (every 10–12 days) to determine the minimum detection limit (MDL) and uncertainty. The MDLs (uncertainties in %) for the IC analysis were 0.06 μg m^{-3} (5.18%) for Cl^-, 0.13 μg m^{-3} (5.06%) for NO_3^-, 0.15 μg m^{-3} (3.25%) for SO_4^{2-}, 0.21 μg m^{-3} (6.57%) for Na^+, 0.05 μg m^{-3} (4.81%) for NH_4^+, 0.08 μg m^{-3} (17.8%) for K^+, 0.10 μg m^{-3} (12.1%) for Ca^{2+}, and 0.04 μg m^{-3} (22.6%) for Mg^{2+}. The average Li^+ and Br^- concentrations were 0.029 ± 0.005 and 0.031 ± 0.004 ppb, respectively. These results indicate that the measurement of the WSIIs was maintained under stable and reliable conditions during this study (Zhang et al., 2019a).

2.2.2. Measurement of gaseous substances

Large amounts of gaseous HNO_3 and NH_3 present in the air tend to dissolve in water and are converted to NO_3^- and NH_4^+, which must be removed during sampling because they can lead to overestimation of concentrations in the IC analysis. To accurately measure NO_3^- and NH_4^+ in the inserted samples, two annular denuders (URG Corporation, Chapel Hill, NC, USA), which can remove gaseous precursors (HNO_3 and NH_3), were installed at the front of the PILS. The annular denuders were coated with two solutions to collect gaseous precursors on the glass surface. To collect HNO_3, a coating solution was prepared by adding 5.05 g of sodium carbonate (Na_2CO_3), 4 ml of glycerol ($C_3H_8O_3$), and 250 ml of methanol (CH_3OH) in deionized water. To collect NH_3, a coating solution was prepared by adding 100 ml of deionized water and 6.26 ml of phosphoric acid (H_3PO_4) to 900 ml of methanol.

To observe gaseous precursors (HNO_3, sulfur dioxide (SO_2), NH_3, and carbon dioxide (CO)), sampling was performed during the summer 2018 measurement period in Seongbuk and the spring 2019 measurement period in Jungnang, using an ammonia analyzer EAA-30r-EP (Los Gatos Research, USA), a 48i gas filter correlation (GFC) CO analyzer (Model 48i, Thermo Scientific, USA), a UV fluorescence method (MEZUS-110, KENTEK, Korea) for SO_2, and the parallel-plate diffusion scrubber ion chromatography (PPDS-IC; Metrohm) technique for HNO_3 (Table 1). NH_3 measurements were performed such that the inlet tubing

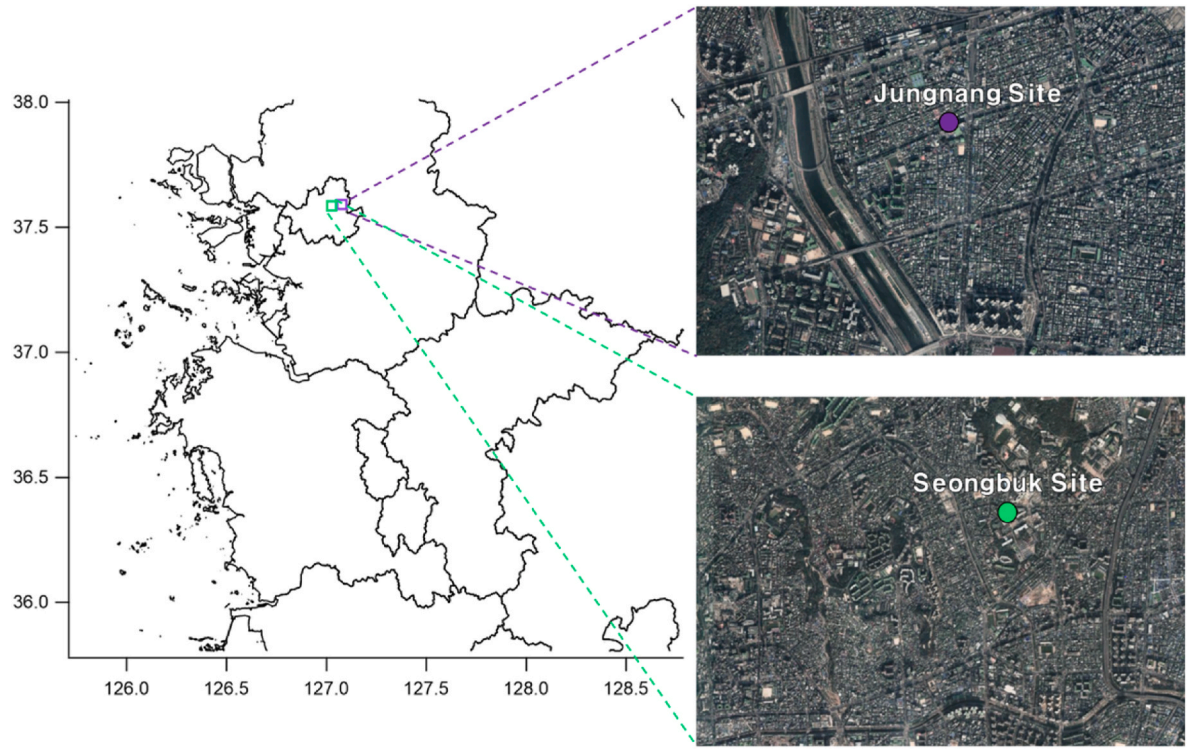

Fig. 1. Locations of the sampling sites; operated in Seongbuk (Korea University, 37.585949 °N, 127.025420 °E) during the summer of 2018 (from June 1 to August 22, 2018) and Jungnang (KT plaza branch, 37.589729 °N, 127.079042 °E) during the spring of 2019 (from March 29 to May 31, 2019).

Table 1
The instruments used for the measurement of gas and particle phases.

Phase	Instrument	Manufacturer	Species
Gas	EAA-30r-EP	Los Gatos Research (USA)	NH_3
	MEZUS 110	KENTEK (USA)	SO_2
	T500U	Teledyne (USA)	NOx (NO, NO_2)
	PPDS-IC	Metrohm (Switzerland)	HNO_3
	48i	Thermo scientific (USA)	CO
Particle	T640	Teledyne (USA)	PM_{10}, $PM_{2.5}$
	PILS-IC	Metrohm (Switzerland)	Inorganic ions (NO_3^-, SO_4^{2-}, Cl^-, NH_4^+, Na^+, Ca^{2+}, K^+, Mg^{2+})

temperature was maintained at 45 °C to reduce the degree of NH_3 adsorption to the tubing (Kim et al., 2021a).

2.3. Conditional probability function (CPF) analysis

A conditional probability function (CPF) analysis was conducted to identify the inflow paths and sources of pollutants at the sampling sites. This technique simultaneously identifies the direction of the main emission sources in a CPF and provides information regarding their dispersion in bivariate polar coordinates (Uria-Tellaetxe and Carslaw, 2014; Kim et al., 2018). A CPF is generally used to identify the sources of local pollution (Jain et al., 2020; Kanchanasuta et al., 2020). Uria--Tellaetxe and Carslaw (2014) identified high-concentration emission sources using CPF results, where the concentrations of pollution sources above the 75th percentile were selected.

3. Results and discussion

3.1. Characteristics of $PM_{2.5}$ in Seoul's atmosphere

3.1.1. Chemical composition of $PM_{2.5}$

Water-soluble inorganic ionic components were observed during the summer measurement period in Seongbuk from June 1 to August 22, 2018, and the spring measurement period in Jungnang from March 29 to May 31, 2019 (Table 2). All results are shown for the WSIIs of $PM_{2.5}$, except for the organics. The composition of WSIIs in the $PM_{2.5}$, for the known species (nitrate, sulfate, ammonium, and crustal elements) from the IC measurement is shown in Fig. 2. Both sampling sites had relatively low concentrations compared to those recorded in previous studies at different sites (Table 2). For example, a sampling site in Jongno (Park et al., 2020a), found in the center of Seoul (37.58 °N, 127.00 °E), is enclosed by various sources of pollutant emissions. Another site in Eunpyeong, located on the rooftop of a building in Northwest Seoul (Park et al., 2018), is situated 67 m above the ground and represented an urban monitoring site in Bulkwang, Seoul (37.610646 °N, 126.933707 °E). Gwangjin, as listed in Table 2, is located on the north side of the Han River in Seoul in the large water purification system of Gwangjin, which is enclosed by commercial and residential buildings (37.547080 °N, 127.092492 °E) (Shon et al., 2012; Son et al., 2012). Kim et al. (2007) collected samples from the rooftop of the Graduate School of Public Health of Seoul National University in Jongno, Seoul (approximately 17 m above the ground, 37.464871 °N, 126.954736 °E). Overall, the results of all studies listed in Table 2 showed that higher concentration of $PM_{2.5}$ and nitrate, and a lower concentration of sulfate, were found in spring, in comparison to summer. It was considered that the lower nitrate in summer was affected by thermal decomposition at high temperatures, and the higher sulfate in summer was attributed to sulfate oxidation from SO_2 under the meteorological conditions of higher temperature and humidity (Khoder, 2002; Chan et al., 2018).

During the 2018 measurement period in Seongbuk, the $PM_{2.5}$ concentration was 18.45 μg m^{-3}, and among the WSII components, the

Table 2
Comparison of $PM_{2.5}$ average concentrations with those of previous studies.

Location	Year	Season	$PM_{2.5}$	NO_3^-	SO_4^{2-}	NH_4^+	Temp	RH	References
			μg m^{-3}	μg m^{-3}	μg m^{-3}	μg m^{-3}	°C	%	
Seongbuk	2018	Summer	18.5 ± 11.5[a,b]	1.9 ± 2.9	4.1 ± 3.2	2.33 ± 1.8	27.8 ± 4.6	54.3 ± 14.7	This study
Jungnang	2019	Spring	22.6 ± 14.3	4.5 ± 5.1	2.9 ± 2.0	2.5 ± 1.8	17.5 ± 5.0	46.8 ± 19.9	
Jongno[c]	2015	Summer	34.1 ± 1.9	4.6 ± 3.2	10.9 ± 2.0	4.6 ± 0.3	27.2 ± 0.9	69.3 ± 5.2	Park et al. (2020a)
		Spring	69.3 ± 11.4	11.2 ± 2.5	9.6 ± 1.46	6.9 ± 1.2	12.9 ± 1.4	54.8 ± 4.7	
Eunpyeong[d]	2011	Summer	19.2 ± 16.4	6.4 ± 5.8	3.7 ± 4.9	4.1 ± 3.7	–	–	Park et al. (2018)
		Spring	28.9 ± 20.0	6.1 ± 6.2	7.2 ± 5.8	4.9 ± 3.7	–	–	
Gwangjin[e]	2010	Summer	22.4 ± 17.3	11.2 ± 4.8	6.3 ± 5.4	3.7 ± 3.6	25.8 ± 3.3	74.8 ± 15.9	Shon et al. (2012)
		Spring	25.5 ± 15.4	13.8 ± 7.2	5.8 ± 4.4	3.9 ± 2.9	11.0 ± 6.6	61.0 ± 19.9	
Gwangjin[e]	2009	Summer	21.3 ± 11.7	2.9 ± 2.0	3.6 ± 2.5	1.9 ± 1.3	–	–	Son et al. (2012)
		Spring	28.8 ± 14.4	4.6 ± 2.0	4.0 ± 2.9	2.5 ± 1.6	–	–	
Jongno[f]	2003–2004	Summer	38.2 ± 1.1	6.6 ± 5.9	8.7 ± 7.1	6.5 ± 5.3	–	–	Kim et al. (2007)
		Spring	46.5 ± 18.5	9.3 ± 7.1	7.3 ± 4.8	5.7 ± 4.6	–	–	

[a] Average ± Standard deviation.
[b] The data from a sampling site located 1 km south of Seongbuk was used instead because $PM_{2.5}$ was not measured in 2018.
[c] Located in the center of Seoul, Korea (37.581 °N, 127.001 °E).
[d] Located in the northwest part of Seoul (37.61 °N, 126.93 °E).
[e] Located on the north side of the Han River of Seoul (37.32 °N, 127.05 °E).
[f] Located on the roof of the Graduate School of Public Health of Seoul National University (37.514 °N, 127.001 °E).

Table 3
The mass concentrations of $PM_{2.5}$, NO_3^-, SO_4^{2-}, NH_4^+ and crustal elements in measurement periods and episodes exceeding the Korean air quality standard (35 μg m^{-3}).

Site	Case	$PM_{2.5}$	NO_3^-	SO_4^{2-}	NH_4^+	Crustal elements[c]
		μg m^{-3}	μg m^{-3}	μg m^{-3}	μg m^{-3}	μg m^{-3}
Seongbuk	Summer	18.45	1.91	4.13	2.33	0.21
	$PM_{2.5}$ over 35 μg m^{-3} [a]	36.39	5.97	5.70	4.46	0.23
Jungnang	Spring	22.60	4.50	2.92	2.54	0.40
	$PM_{2.5}$ over 35 μg m^{-3} [b]	42.31	9.50	4.54	4.12	0.72

[a] June 24 and 25, and July 23, 2018.
[b] April 23 and May 4, 5, 12, 13, 23, and 25, 2019.
[c] $Crustal = Cl^- + K^+ + Ca^{2+} + Na^+ + Mg^{2+}$

SO_4^{2-} concentration was the highest at 4.13 μg m^{-3} (48.1% of the WSII composition) (Fig. 2, Table 3). $PM_{2.5}$ exceeded the air quality standard daily average in Korea (35 μg m^{-3}) for three days (June 24, June 25, and July 23). Among the WSII components, the concentration of SO_4^{2-} increased to 5.70 μg m^{-3}, indicating a decreased composition of 34.8% during the three days. The concentration of NO_3^- was the highest at 5.97 μg m^{-3}, with an increased composition of 36.5%. In 2019, in Jungnang, the $PM_{2.5}$ concentration was 22.58 μg m^{-3}, and among the WSII components, NO_3^- had the highest concentration of 4.50 μg m^{-3} (43.4% of the WSII composition). During this period, $PM_{2.5}$ exceeded the air quality standard daily average in Korea for eight days (April 23 and May 4, 5, 12, 13, 23, 24, and 25). The concentration of NO_3^- increased to 9.50 μg m^{-3}, indicating a decreased composition of 50.4% during the eight days. Finally, the SO_4^2 concentration increased to 4.54 μg m^{-3}, indicating a decreased composition of 24.0%. These results indicate that the measurement periods were characterized by a high concentration of $PM_{2.5}$, from the formation of nitrate compared to sulfate.

3.1.2. *Interactions between PM and gaseous precursors*

The reaction of ammonia with nitric acid (HNO_3) and sulfuric acid (H_2SO_4) contributes to the formation of ammonium nitrate (NH_4NO_3) and ammonium sulfate ($(NH_4)_2SO_4$). Therefore, it is necessary to identify the atmospheric conditions of ammonia in ambient air. Seinfeld and Pandis (2006) reported that the atmospheric conditions of ammonia are restrictive factors for secondary aerosol formation. Under ammonium-rich conditions, the concentration of $PM_{2.5}$ can increase because SO_2 or NOx are continuously generated in the SIA. In this study, ammonium-poor conditions did not cause an immediate increase in the concentration of $PM_{2.5}$, likely owing to its limited reaction with acidic precursors (HNO_3 and H_2SO_4) to generate SIA. However, SIA may also be formed if insufficient ammonia is supplied from other sources or by long-range transport.

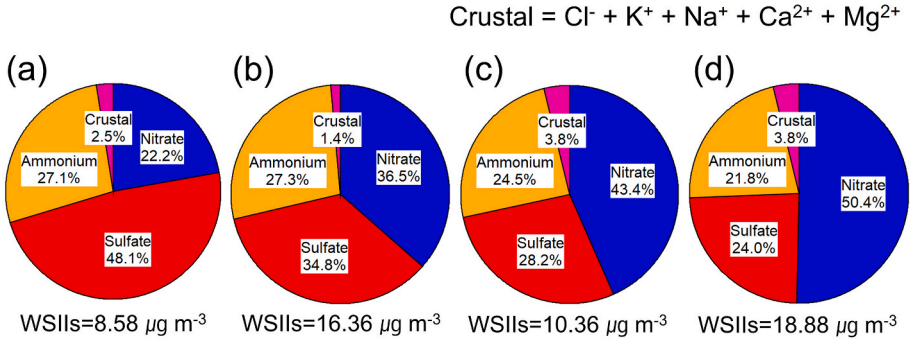

Fig. 2. Chemical compositions of water-soluble inorganic ions (WSIIs) in $PM_{2.5}$ during the entire period and episodes exceeding the Korean air quality standard (35 μg m^{-3}). (a) Seongbuk for the measurement period (from June 1 to August 22, 2018), (b) Seongbuk for the measurement period exceeding the Korean air quality standard, (c) Jungnang for the entire measurement period (from March 29 to May 31, 2019), (d) Jungnang for the measurement period exceeding the Korean air quality standard.

Pathak et al. (2009) reported a change in the molecular ratio of NO_3^- and SO_4^{2-} according to the change in the molecular ratio of NH_4^+ and SO_4^{2-}. When the molecular ratio of NH_4^+ to SO_4^{2-} was 1.5, the production of NH_4NO_3 was apparent through the reaction of the two gaseous substances, NH_3 and HNO_3. Therefore, it was indicated that the main reaction of $[NH_4^+]/[SO_4^{2-}]$ with a ratio below 1.5 is heterogeneous and with a ratio above 1.5 is a homogeneous reaction. The heterogeneous reaction results indicate the preferential reaction of $(NH_4)_2SO_4$ in the aqueous phase, followed by the production of NH_4NO_3. However, the homogeneous reaction results indicate that NH_4NO_3 increased as the concentrations of NH_3 and NO_X increased when H_2SO_4 reacted sufficiently with NH_3 to produce ammonium sulfate $(NH_4)_2SO_4$.

Fig. 3 presents the molar concentrations of NO_3^-, SO_4^{2-}, and NH_4^+ in the atmosphere of Seongbuk, Seoul, in the summer of 2018, indicating mostly ammonium-poor conditions, with some periodic exceptions. However, during that summer, environmental conditions, specifically the high temperature, resulted in the decomposition of NO_3^-. Hence, SO_4^{2-} had the highest percentage of WSIIs during the measurement period (Fig. 2). Therefore, it is possible that the formation of $(NH_4)_2SO_4$ through the heterogeneous reaction of the atmosphere in Seongbuk measured in summer was stronger than that measured in spring(Pathak et al., 2009). There were relatively more NO_3^- and NH_4^+ ions in the atmosphere than SO_4^{2-}; therefore, the conditions were considered to be ammonium-rich. As ammonium-rich conditions have been observed during most previously reported measurement periods, the generation of NH_4NO_3 through homogeneous reactions in the atmosphere is likely strong (Griffith et al., 2015).

The molar ratio (R) and SNA values were used to identify the possibility of NO_3^- formation (Fig. 4). The calculation of the R-value in this study is given by Eq. (1). Xu et al. (2019) reported that the formation of NO_3^- was suppressed by the reduction of ammonia owing to ammonia limitation ($R < 1$) and a decrease in nitric acid owing to nitric acid limitation ($R > 1$). The R-value was 60% of the HNO_3 limitation and 40% of the NH_3 limitation in Seongbuk (2018). In Jungnang (2019), the R-value was calculated as 74% for HNO_3 limitation and 26% for NH_3 limitation. The formation of NO_3^- was likely suppressed by the reduction of HNO_3. However, because hydrochloric acid (HCl) was not measured during the measurement period, its concentration was not considered in the R values, and it is possible that these R values resulted in overestimation(Xu et al., 2019).

$$R = \frac{NH_3(g) + NH_4^+}{2SO_4^{2-} + NO_3^- + HNO_3(g) + Cl^- + HCl(g) - 2Ca^{2+} - K^+ - 2Mg^{2+}} \quad (1)$$

Fig. 5 shows the changes in the measured constant values (K_m) and the theoretical equilibrium constant (K_p) of NH_4NO_3 to confirm whether the environment was suitable for the formation of NH_4NO_3 during the entire measurement period. The calculations for K_p and K_m in this study are shown in Eqs. (2) and (3), respectively. Here, the relative humidity was assumed to be solid NH_4NO_3 under the condition that the relative humidity was less than the deliquescence relative humidity and K_p was simplified. In Eq. (2), T is the absolute temperature (K) and K_p is the unit of $ppbv^2$ (Li et al., 2014).

$$\ln K_p = 84.6 - 24220 / T - 6.1 \times \ln(T / 298) \quad (2)$$

$$K_m = [NH_3] \times [HNO_3] \quad (3)$$

In Seongbuk (2018), the NH_3 and HNO_3 were 13.08 (±5.26) and 0.53 (±0.32) ppb, respectively, at a temperature of 27.3 (±4.8) °C. In Jungnang (2019), the NH_3 and HNO_3 were 14.87 (±4.18) ppb and 0.63 (±0.36) ppb, with a temperature of 18.3 (±5.1) °C. During the 2018 measurement period in Seongbuk, the NH_3 and HNO_3 concentrations were relatively low and the temperature was higher than that in Jungnang in 2019. Hence, most of the measured constant values (K_m) were below the solid line (K_p). In July and August 2018, when high temperatures continued, SO_4^{2-} concentrations increased and the environment was NH_3-limited; therefore, it is likely that $(NH_4)_2SO_4$ was produced first, after which NH_3 was consumed in the formation of NH_4NO_3 and $(NH_4)_2SO_4$ (Stelson et al., 1979). During the 2019 measurement period in Jungnang, most K_m values were higher than, and closer to K_p. This suggests that conditions such as NH_3 and HNO_3 concentrations and temperature were suitable for the formation of NH_4NO_3 (Li et al., 2014). As the atmospheric conditions in Jungnang were HNO_3-limited, if K_m was lower than K_p through HNO_3 reduction, NO_3^- formation was likely suppressed. However, there is some uncertainty because neither the influence of the components of $PM_{2.5}$, nor relative humidity was considered.

3.2. Estimation of urban high-concentration $PM_{2.5}$ sources

3.2.1. Conditional probability function analysis

During the research period, wind direction and speed were measured using an automatic weather system (AWS). The wind directions in the

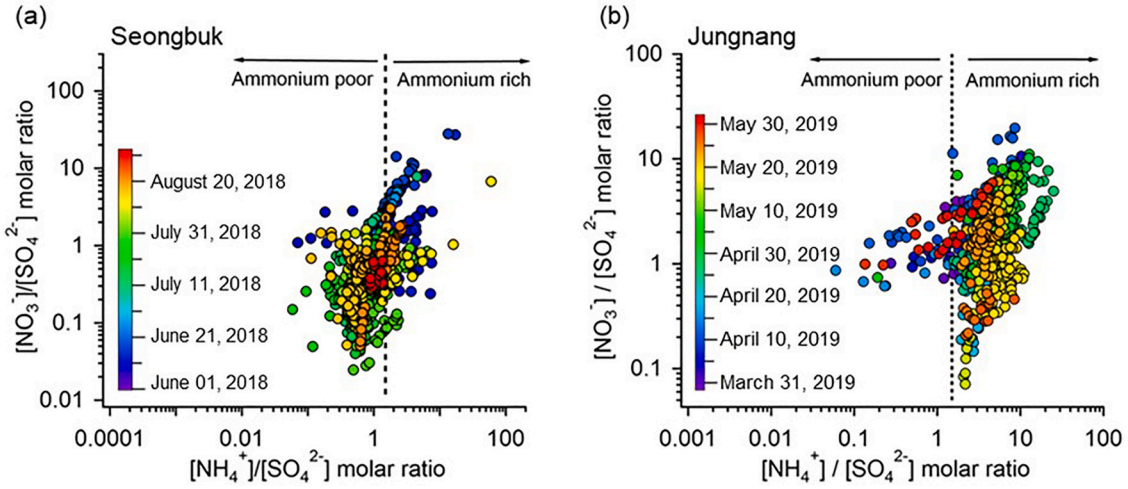

Fig. 3. The molar concentrations of NO_3^-, SO_4^{2-}, and NH_4^+ at Seoul. The gray dashed line indicates the value of nitrate formation separating ammonium-poor and ammonium-rich conditions, that is, a ratio of 1.5 for $[NH_4^+]/[SO_4^{2-}]$ via the gas-phase reaction between ammonia, nitric acid, and ammonium nitrate (Pathak et al., 2009).

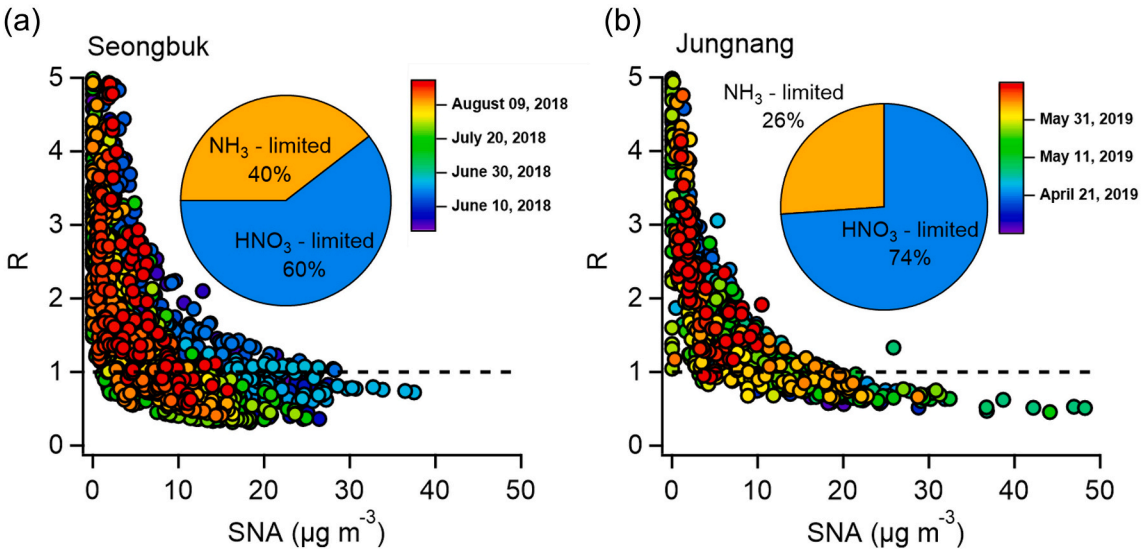

Fig. 4. Molar ratio (R) and concentrations of the SNA (sulfate + nitrate + ammonium) at (a) Seongbuk (2018) and (b) Jungnang (2019).Composition of HNO_3^- and NH_3^-limited during the same period.

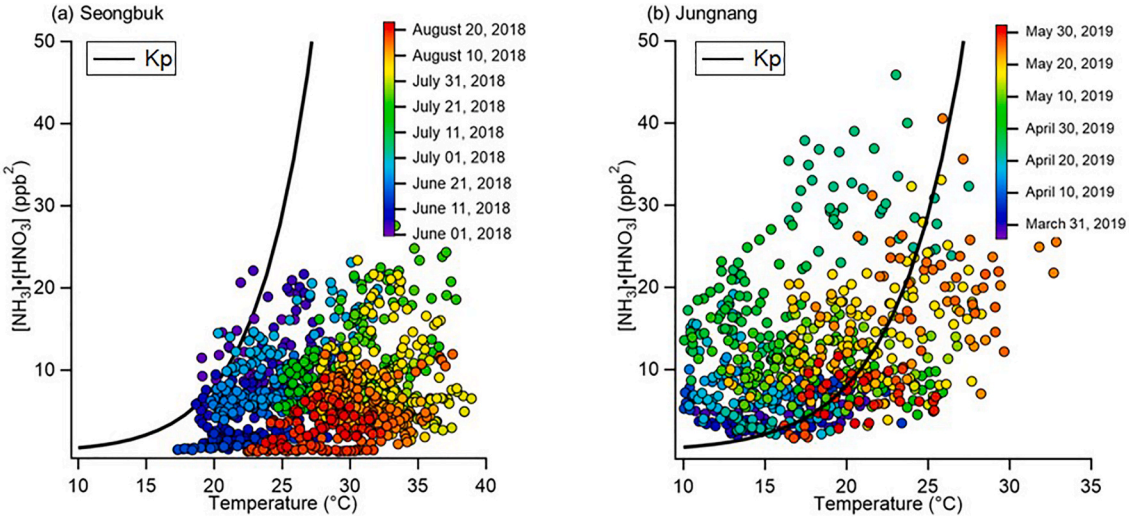

Fig. 5. Comparison of the concentrations of products of HNO_3 and NH_3 with the theoretical equilibrium constant in (a) Seongbuk and (b) Jungnang.

spring in Jungnang were mainly from the west, and the average wind speeds at both sampling sites were similar, at 2.05 m s^{-1}. Because Seongbuk was measured during the summer, the high average temperature and relative humidity promoted the thermal decomposition of NO_3^- and SO_4^{2-} because of the aqueous oxidation of SO_2. Such conditions render the analysis of emission sources difficult; therefore, only the spring period in Jungnang was considered for CPF and cluster analysis (Khoder, 2002; Wang et al., 2016).

As shown in Fig. 6, during the 2019 measurement period in Jungnang, the main emission sources of $PM_{2.5}$, NO_3^-, and CO were identified as coming from the southwest (wind speed of 1.5–2.0 m s^{-1}) and the west (wind speed of 3.5–4.0 m s^{-1}). In winds with speeds of 1.5–2.0 m s^{-1}, the concentration ranges of $PM_{2.5}$, NO_3^-, and CO were 43–92 μg m^{-3}, 10–36 μg m^{-3}, and 642–1003 ppb, respectively. In winds with a speed of 3.5–4.0 m s^{-1}, the concentration ranges of $PM_{2.5}$, NO_3^-, CO, and SO_4^{2-} were 33–38 μg m^{-3}, 6–8 μg m^{-3}, 454–514 ppb, and 5–16 μg m^{-3} respectively. Sulfate (SO_4^{2-}) and SO_2 emission sources located in the west and southwest were the most significant contributors to the high concentrations, and they were estimated to be generated over a larger area than the other pollution sources. Furthermore, it seems that the long-range transport of air pollutants from China also affected Seoul, along with pollutants emitted from industrial complexes located in the metropolitan area (Fig. 6).

3.2.2. *Polar annulus plot analysis*

To examine the temporal changes in concentration according to the wind direction for each pollution source, the 2019 measurement period in Jungnang was visualized concerning the time and day of each week through a polar annulus plot (Fig. 7). A polar annulus plot was used to visualize the average concentration of pollutants and how the concentrations varied with time by color mapping wind direction as a continuous surface (Harrison et al., 2012; Masiol et al., 2017). As shown in Fig. 7b, the NO_3^- concentration reached its maximum in dawn when the insolation increased and showed a flow in all directions. This phenomenon is a known characteristic of urban environments in spring. As surface temperatures decrease, NO_3^- concentration in lower boundary layer height increases. In addition, nitrogen dioxide (NO_2) is converted to NO_3^- by photochemical reactions, thus increasing its concentration (Wang et al., 2019). After 10 a.m., the NO_3^- concentration decreased because of the rising mixed layer and increasing temperature. During the

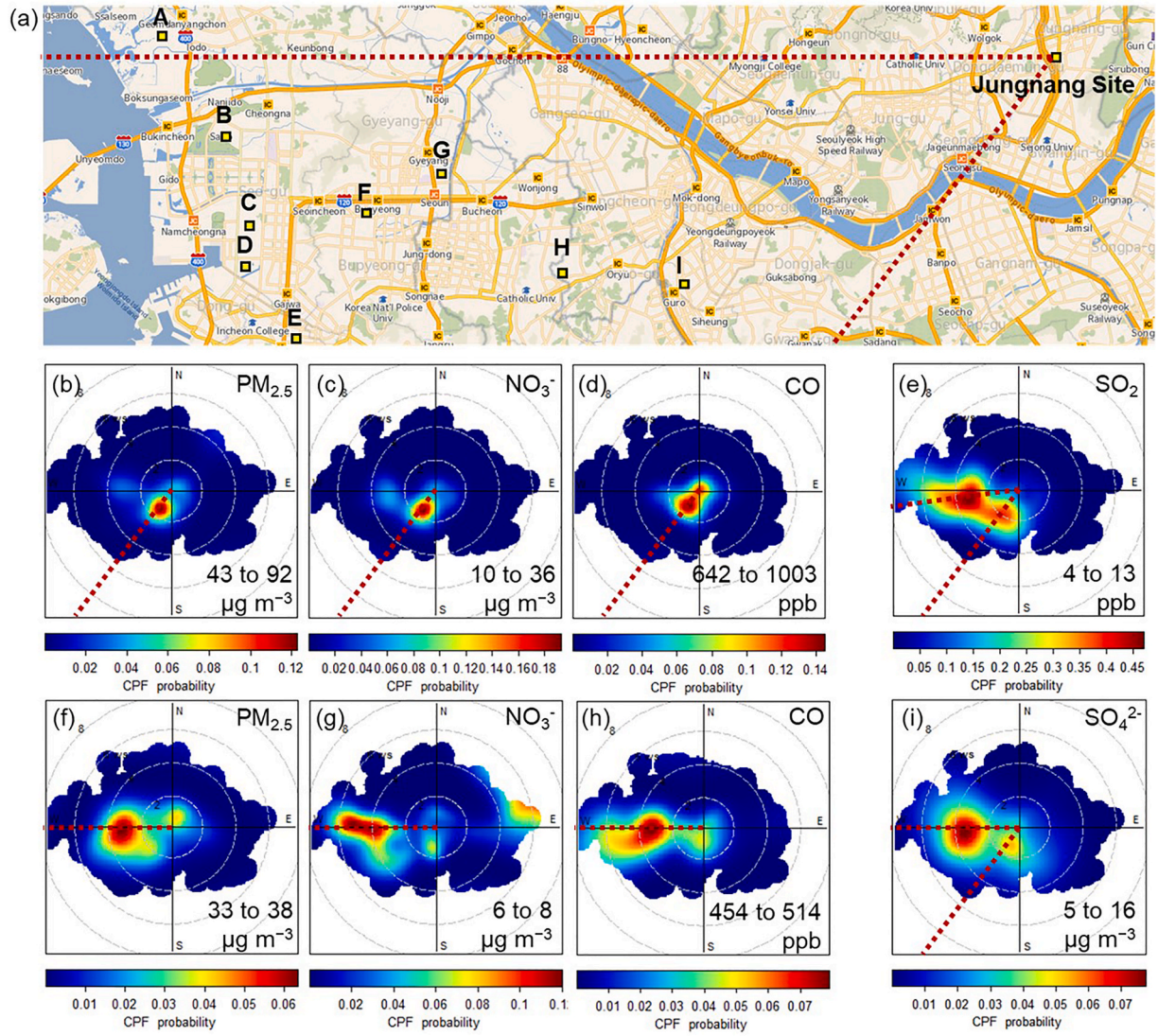

Fig. 6. (a) Location of the major industrial facilities (A: Hakun Industrial Complex, B: Incheon West Regional Industrial Complex, C: Petrochemical plant, D: Incheon Machinery Industrial Complex, E: Juan National Industrial Complex, F: Bupyeong National Industrial Complex, G: Location of Seoun industrial complex, H: Onsu General Industry Complex, I: Seoul Digital National Industrial Complex) in the Seoul metropolitan area (SMA) and Jungnang, (b–i) Results of conditional probability function (CPF) analysis of $PM_{2.5}$, nitrate, sulfate, CO, and SO_2.

measurement period, high concentrations of $PM_{2.5}$, NO_3^-, CO, SO_2, and NO_2 were observed in the air flowing southwest in the morning. In this study, air from the southwest was estimated to flow through central Seoul, leading to higher concentrations here than those in other areas (Fig. 6a). According to previous research, due to the increase in CO and NO_2 concentrations, which are from local sources, there were more dominant NO_3^- sources than photochemical sources in the high-concentration cases, and atmospheric stagnation led to the accumulation and inflow of high concentrations of pollutants (Kim et al., 2022). Seoul reported it is a major emission source of urban air pollutants such as CO and NO_2 (Seo et al., 2018). The NO_X supplied to the atmosphere by vehicles in Jung-gu (downtown) and the southwest, which is located on the Jungnangcheon and Dongbu Expressways from Jungnang, is likely to contribute to the increase in NO_3^- concentration on Saturdays.

High concentrations of pollutants flowing from west of Jungnang were observed mainly in the afternoon (Fig. 7). Sulfate (SO_4^{2-}) flowed over a larger area than NO_3^-, mainly originating from the west, at relatively high concentrations (Fig. 7b and c). Low-concentration $PM_{2.5}$ and relatively high wind speeds were observed flowing from the southwest (Fig. 7a and g). These results were possibly influenced by the Incheon industrial complex, which is located approximately 35 km west of Jungnang, and long-range transport from China (Kim et al., 2016, 2018d).

3.2.3. *Cluster analysis*

To confirm the air trajectories during the measurement period, 72-h backward trajectories in spring from March 29 to May 31, 2019, were calculated using the HYSPLIT model (https://www.arl.noaa.gov/hysplit/). Meteorological data from the Global Data Assimilation System were used, and the modeling point was analyzed at an altitude of 500 m at the KT Plaza Jungnang sampling site (14 m above sea level, 37.590889 °N, and 127.078232 °E).

According to the cluster analysis, in Korea, inflow from inland atmospheric stagnation (navy) contributed to 27.2%, with most inflows from the east coast of China (orange and blue), North China (green), and Mongolia (brown) during this period (Fig. 8). Because of the concentration of large ports, petrochemical plants, and thermal power plants in East China (comprising Shandong, Jiangsu, Zhejiang, and Fujian), it is necessary to consider the impact of coal and oil combustion (Kim et al.,

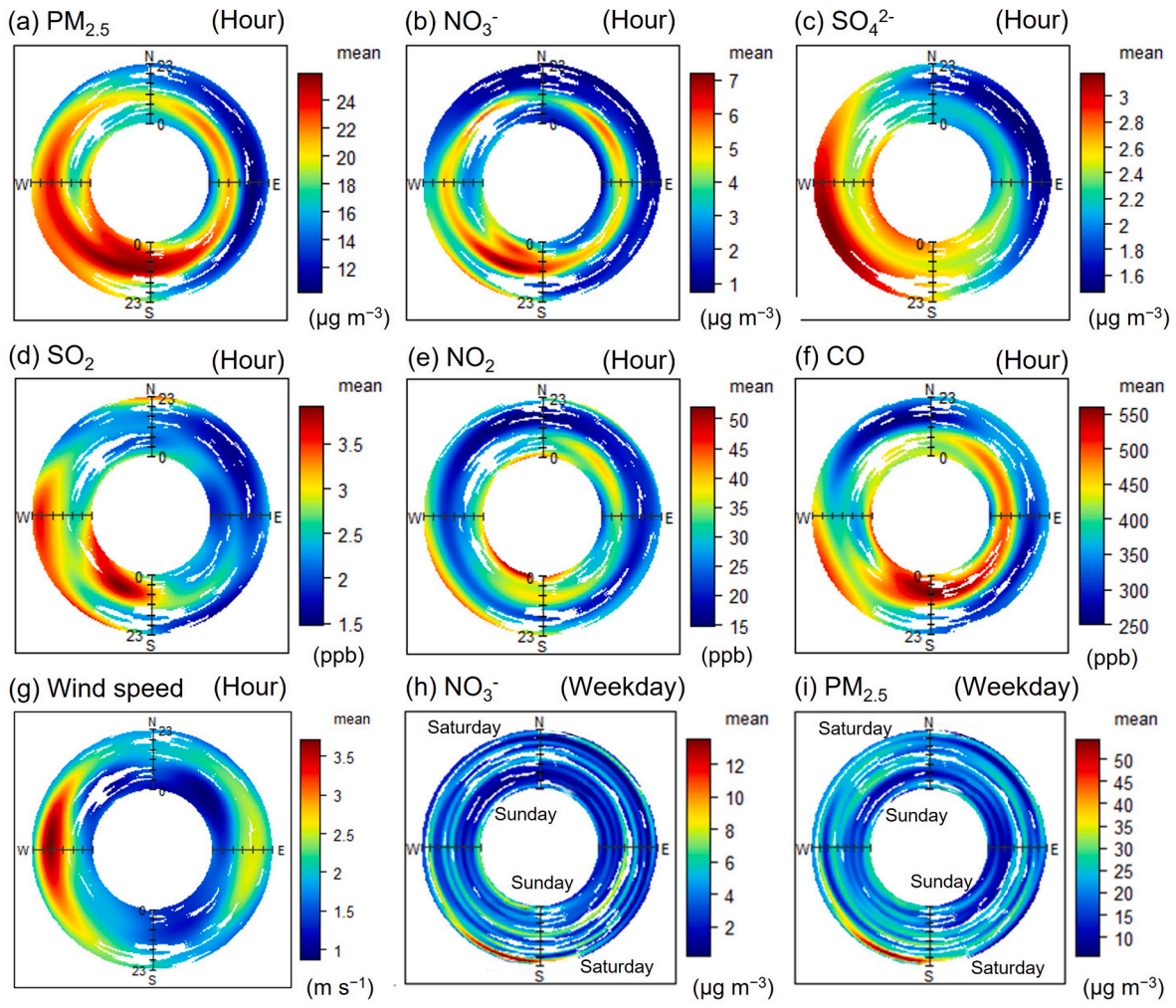

Fig. 7. The polar annulus plot analysis for Jungnang, visualizing the concentration of pollutants in terms of wind direction using color mapping. The results indicate how pollutant concentrations vary overtime.

2021b) and offshore ship emissions (Ledoux et al., 2018). The average annual $PM_{2.5}$ concentration was four to twelve times higher than that of major cities in developed countries such as Los Angeles, USA (Luo et al., 2018; Bie et al., 2021). A previous study on high concentrations of $PM_{2.5}$ found that 40% of the increase in secondary aerosols in Korea during westerly winds was attributable to East China (Kim et al., 2009). Researchers have also identified through an isotope analysis that SO_4^{2-} was generated from coal combustion in China (Kim et al., 2018c). Furthermore, emissions from China were found to have an annual average impact of 40% on $PM_{2.5}$ concentrations in Seoul. The impact of emissions from China on NO_3^- concentrations in Seoul was as high as 67% in spring (Bae et al., 2020). Therefore, these studies suggest the possibility that some pollutants are influenced by emissions in China.

4. Conclusions

In this study, the concentrations of PM and gaseous precursors were measured during the summers of 2018 and 2019 in Seongbuk and Jungnang, Seoul, respectively. Interaction analysis was conducted on the composition of PM and measurements of its gaseous precursors from sampling sites in Seongbuk and Jungnang, and the characteristics of air quality in Seoul were discussed. This study also traced the emission sources of pollution in Seoul through various analyses during spring. The main conclusions are as follows.

In Seongbuk, SO_4^{2-} had the highest concentration of 4.13 μg m^{-3} (48.1% of WSIIs), and in Jungnang, NO_3^- had the highest concentration of 4.50 μg m^{-3} (43.4% of WSIIs). This was affected by the thermal decomposition of NO_3^- and oxidation of sulfate from SO_2 in the summer. In both spring and summer, the NO_3^- concentration was highest when the $PM_{2.5}$ concentration exceeded the air quality standard in Korea (35 μg m^{-3}). This was attributed to the high concentration of $PM_{2.5}$, which resulted from the formation of nitrate.

Seongbuk exhibited mostly ammonium-poor conditions, with notable production of $(NH_4)_2SO_4$ through a heterogeneous reaction. This likely remained as HNO_3 in the atmosphere because of the high temperatures during the summer measurement period. Jungnang was measured during the spring and mostly exhibited ammonium-rich conditions, with notable production of NH_4NO_3 through a homogeneous reaction. Atmospheric conditions at the Jungnang sampling site promoted the conversion of HNO_3 to NO_3^-. During the measurement period in Jungnang, the atmospheric conditions were mostly HNO_3-limited. It appears that NO_3^- formation was suppressed by the reduction of HNO_3 via the homogeneous reaction of NH_4NO_3. In Seongbuk, it was difficult to locate pollution sources because of NO_3^- decomposition and extensive SO_4^{2-} formation owing to the high average temperature and relative humidity. In Jungnang, high concentrations of $PM_{2.5}$ and NO_3^- in the pollutants originating from the southwest were observed at dawn, probably related to atmospheric stagnation, and the mixing of NO_3^- in lower planetary boundary layer height, due to an decrease in surface temperature. Pollutants flowing from the southwest showed high concentrations on Saturdays, indicating that heavy traffic volume on Fridays had an effect. It is estimated that NO_3^- or SO_4^{2-} generated by

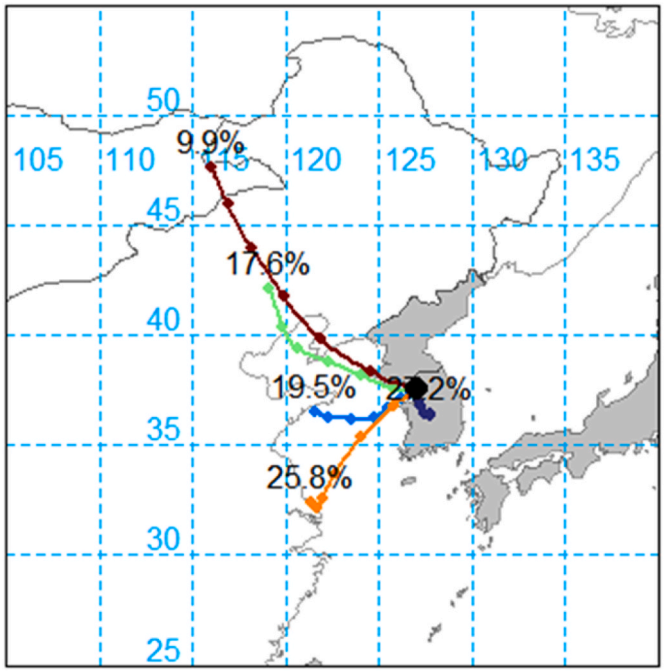

Fig. 8. Backward trajectories of five clusters in Jungnang during spring (from March 29 to May 31), 2019.

photochemical reactions were affected by many industrial facilities located approximately 35 km west of Jungnang. According to the cluster analysis of the Jungnang measurement period, air trajectories were primarily from China. This result suggests that a portion of the pollutants generated in China can affect Korea and are mixed with local sources in Korea, contributing to the increase in pollutant concentrations.

Credit author statement

Seokwon Kang and Taehyun Park: conceptualization, formal analysis, visualization, investigation, writing - original draft, writing - review & editing; Jihee Ban and Kyunghoon Kim: conceptualization, methodology, visualization, investigation, writing - original draft; Rahul Singh and Gyutae Park: investigation, software; Myeong-Bok Kim and Dong-Gil Yu: methodology, investigation; Joo-Ae Kim and Yu-Woon Jang: investigation; methodology, visualization; Sang-Sub Ha and Sang-Woo Kim: visualization, investigation; Moon-Soo Park and Cheol-Hee Kim: software, writing - review & editing; Meehye Lee and Gookyoung Heo: writing - review & editing; Taehyoung Lee: conceptualization, writing - review & editing, supervision.

Declaration of competing interest

The authors declare that they have no known competing financial interests or personal relationships that could have appeared to influence the work reported in this paper.

Acknowledgments

This study was performed at the National Institute of Environment Research (NIER), funded by the Ministry of Environment (MOE) of the Republic of Korea (NIER-2018-22-53-001, NIER-2019-21-06-001). The authors are grateful to the NIER for financial support. We thank the Korea Basic Science Institute (National Research Facilities and Equipment Center) for their financial assistance during the data-processing period. The extended experiment was conducted byKorea Basic Science Institute (National research Facilities and Equipment Center) grant funded by the Ministry of Education (2019R1A6C1020041).

References

Bae, C., Kim, B.U., Kim, H.C., Yoo, C., Kim, S., 2020. Long-range transport influence on key chemical components of PM2.5 in the Seoul Metropolitan Area, South Korea, during the years 2012–2016. Atmosphere 11 (1), 48.
Begam, G.R., Vachaspati, C.V., Ahammed, Y.N., Kumar, K.R., Reddy, R.R., Sharma, S.K., Saxena, M., Mandal, T.K., 2017. Seasonal characteristics of water-soluble inorganic ions and carbonaceous aerosols in total suspended particulate matter at a rural semi-arid site, Kadapa (India). Environ. Sci. Pollut. Res. 24, 1719–1734.
Bie, S., Yang, L., Zhang, Y., Huang, Q., Li, J., Zhao, T., Zhang, X., Wang, P., Wang, W., 2021. Source appointment of PM2.5 in qingdao port, east of China. Sci. Total Environ. 755, 142456.
Chan, E.A.W., Gantt, B., McDow, S., 2018. The reduction of summer sulfate and switch from summertime to wintertime PM2.5 concentration maxima in the United States. Atmos. Environ. 175, 25–32.
Charlson, R.J., Schwartz, S.E., Hales, J.M., Cess, R.D., Coakley, J.A., Hansen, J.E., Hofmann, D.J., 1992. Climate forcing by anthropogenic aerosols. Science 255, 423–430.
Chen, W.-R., Singh, A., Pani, S.K., Chang, S.-Y., Chou, C.C.K., Chang, S.-C., Chuang, M.-T., Lin, N.-H., Huang, C.-H., Lee, C.-T., 2021. Real-time measurements of PM2.5 water-soluble inorganic ions at a high-altitude mountain site in the western North Pacific: impact of upslope wind and long-range transported biomass-burning smoke. Atmos. Res. 260, 105686.
Cheng, C., Shi, M., Liu, W., Mao, Y., Hu, J., Tian, Q., Chen, Z., Hu, T., Xing, X., Qi, S., 2021. Characteristics and source apportionment of water-soluble inorganic ions in PM2.5 during a wintertime haze event in Huanggang, central China. Atmos. Pollut. Res. 12, 111–123.
Do, T.V., Vuong, Q.T., Choi, S.-D., 2021. Day–night variation and size distribution of water-soluble inorganic ions in particulate matter in Ulsan, South Korea. Atmos. Res. 247, 105145.
Griffith, S.M., Huang, X.H., Louie, P.K.K., Yu, J.Z., 2015. Characterizing the thermodynamic and chemical composition factors controlling PM2.5 nitrate: insights gained from two years of online measurements in Hong Kong. Atmos. Environ. 122, 864–875.
Guo, W., Zhang, Z., Zheng, N., Luo, L., Xiao, H., Xiao, H., 2020. Chemical characterization and source analysis of water-soluble inorganic ions in PM2.5 from a plateau city of Kunming at different seasons. Atmos. Res. 234, 104687.
Harrison, R.M., Laxen, D., Moorcroft, S., Laxen, K., 2012. Processes affecting concentrations of fine particulate matter (PM2.5) in the UK atmosphere. Atmos. Environ. 46, 115–124.
He, Q., Yan, Y., Guo, L., Zhang, Y., Zhang, G., Wang, X., 2017. Characterization and source analysis of water-soluble inorganic ionic species in PM2.5 in Taiyuan city, China. Atmos. Res. 184, 48–55.
Intergovernmental Panel on Climate Change (IPCC), 2007. Climate Change 2007: the Physical Science Basis. Contribution of Working Group I to the Fourth Assessment Report of the IPCC.
Jain, S., Sharma, S.K., Vijayan, N., Mandal, T.K., 2020. Seasonal characteristics of aerosols (PM2.5 and PM10) and their source apportionment using PMF: a four year study over Delhi, India. Environ. Pollut. 262, 114337.
Jo, Y.-J., Lee, H.-J., Jo, H.-Y., Woo, J.-H., Kim, Y., Lee, T., Heo, G., Park, S.-M., Jung, D., Park, J., Kim, C.-H., 2020. Changes in inorganic aerosol compositions over the Yellow Sea area from impact of Chinese emissions mitigation. Atmos. Res. 240, 104948.
Kanchanasuta, S., Sooktawee, S., Patpai, A., Vatanasomboon, P., 2020. Temporal variations and potential source areas of fine particulate matter in bangkok, Thailand. Air Soil. Water Res. 13, 1178622120978203.
Kang, S., Park, G., Park, T., Ban, J., Kim, K., Seo, Y., Choi, J., Seo, S., Choi, J., Bae, M.S., Lee, T., 2020. Semi-continuous measurements of water-soluble organic carbon and ionic composition of PM2.5 in baengnyeong island during the 2016 KORUS-AQ (Korea-United States air quality study). Asian J. Atmos. Environ. 14 (3), 307–318.
Khoder, M.I., 2002. Atmospheric conversion of sulfur dioxide to particulate sulfate and nitrogen dioxide to particulate nitrate and gaseous nitric acid in an urban area. Chemosphere 49 (6), 675–684.
Kim, B.U., Kim, O., Kim, H.C., Kim, S., 2016. Influence of fossil-fuel power plant emissions on the surface fine particulate matter in the Seoul Capital Area, South Korea. J. Air Waste Manag. Assoc. 66 (9), 863–873.
Kim, H.S., Huh, J.B., Hopke, P.K., Holsen, T.M., Yi, S.M., 2007. Characteristics of the major chemical constituents of PM2.5 and smog events in Seoul, Korea in 2003 and 2004. Atmos. Environ. 41 (32), 6762–6770.
Kim, K., Park, G., Kang, S., Singh, R., Song, J., Choi, S., Park, I., Yu, D.G., Kim, M.B., Bae, M.S., Jung, S., Chang, Y., Park, J., Jung, H.J., Lim, Y.J., Lee, T., 2021a. The comparisons of real-time ammonia adsorption measurement in varying inlet tubes and the different ammonia measurement methods in the atmosphere. Asian J. Atmos. Environ 15 (4), 93–102.
Kim, N.K., Kim, I.S., Song, I.H., Park, S.M., Lim, H.B., Kim, Y.P., Shin, H.J., Lee, J.Y., 2021b. Temporal variation of sulfate concentration in PM2.5 and major factors enhancing sulfate concentration in the atmosphere of Seoul, Korea. Air Qual. Atmos. Health 14, 985–999.
Kim, S., Kim, T.Y., Yi, S.M., Heo, J., 2018. Source apportionment of PM2.5 using positive matrix factorization (PMF) at a rural site in Korea. J. Environ. Manag. 214, 325–334.
Kim, Y., Kim, H., Kang, H., de Foy, B., Zhang, Q., 2022. Impacts of secondary aerosol formation and long-range transport on severe haze during the winter of 2017 in the Seoul metropolitan area. Sci. Total Environ. 804, 149984.

Kim, Y.J., Woo, J.H., Ma, Y.I., Kim, S., Nam, J.S., Sung, H., Choi, K.C., Seo, J., Kim, J., Kang, C.H., Lee, G., Ro, C.U., Chang, K., Sunwoo, Y., 2009. Chemical characteristics of long-range transport aerosol at background sites in Korea. Atmos. Environ. 43 (34), 5556–5566.

Kim, Y., Lee, I., Lim, C., Farquhar, J., Lee, S.M., Kim, H., 2018c. The origin and migration of the dissolved sulfate from precipitation in Seoul, Korea. Environ. Pollut. 237, 878–886.

Kim, Y., Seo, J., Kim, J.Y., Lee, J.Y., Kim, H., Kim, B.M., 2018d. Characterization of PM2.5 and identification of transported secondary and biomass burning contribution in Seoul, Korea. Environ. Sci. Pollut. Res. 25 (5), 4330–4343.

Lang, J., Zhang, Y., Zhou, Y., Cheng, S., Chen, D., Guo, X., Chen, S., Li, X., Xing, X., Wang, H., 2017. Trends of PM2.5 and chemical composition in beijing, 2000–2015. Aerosol Air Qual. Res. 17 (2), 412–425.

Ledoux, F., Roche, C., Cazier, F., Beaugard, C., Courcot, D., 2018. Influence of ship emissions on NOx, SO2, O3 and PM concentrations in a North-Sea harbor in France. J. Environ. Sci. 71, 56–66.

Lee, S., Han, C., Ahn, J., Han, Y., Lee, A.-h., Ro, S., Hong, S., 2022. Characterization of trace elements and Pb isotopes in PM2.5 and isotopic source identification during haze episodes in Seoul, Korea. Atmos. Pollut. Res. 13, 101442.

Li, Y., Schwandner, F.M., Sewell, H.J., Zivkovich, A., Tigges, M., Raja, S., Holcomb, S., Molenar, J.V., Sherman, L., Archuleta, C., Lee, T., Collett, J.L., 2014. Observations of ammonia, nitric acid, and fine particles in a rural gas production region. Atmos. Environ. 83, 80–89.

Lin, G.-Y., Chen, H.-W., Chen, B.-J., Chen, S.-C., 2022. A machine learning model for predicting PM2.5 and nitrate concentrations based on long-term water-soluble inorganic salts datasets at a road site station. Chemosphere 289, 133123.

Luo, Y., Zhou, X., Zhang, J., Xiao, Y., Wang, Z., Zhou, Y., Wang, W., 2018. PM2.5 pollution in a petrochemical industry city of northern China: seasonal variation and source apportionment. Atmos. Res. 212, 285–295.

Masiol, M., Hopke, P.K., Felton, H.D., Frank, B.P., Rattigan, O.V., Wurth, M.J., LaDuke, G.H., 2017. Source apportionment of PM2.5 chemically speciated mass and particle number concentrations in New York City. Atmos. Environ. Times 148, 215–229.

McConnell, R., Berhane, K., Gilliland, F., Molitor, J., Thomas, D., Lurmann, F., Avol, E., Gauderman, W.J. Peters J.M., 2003. Prospective study of air pollution and bronchitic symptoms in children with asthma. Am. J. Respir. Crit. Care Med. 168 (7), 790–797.

Pathak, R.K., Wu, W.S., Wang, T., 2009. Summertime PM2.5 ionic species in four major cities of China: nitrate formation in an ammonia-deficient atmosphere. Atmos. Chem. Phys. 9, 1711–1722.

Park, E.H., Heo, J., Kim, H., Yi, S.M., 2020a. Long term trends of chemical constituents and source contributions of PM2.5 in Seoul. Chemosphere 251, 126371.

Park, E.H., Heo, J., Kim, H., Yi, S.M., 2020b. The major chemical constituents of PM2.5 and airborne bacterial community phyla in Beijing, Seoul, and Nagasaki. Chemosphere 254, 126870.

Park, J., Kim, H., Kim, Y., Heo, J., Kim, S.-W., Jeon, K., Yi, S.-M., Hopke, P.K., 2022. Source apportionment of PM2.5 in Seoul, South Korea and Beijing, China using dispersion normalized PMF. Sci. Total Environ. 833, 155056.

Park, S.M., Song, I.H., Park, J.S., Oh, J., Moon, K.J., Shin, H.J., Ahn, J.Y., Lee, M.D., Kim, J., Lee, G., 2018. Variation of PM2.5 chemical compositions and their contributions to light extinction in Seoul. Aerosol Air Qual. Res. 18 (9), 2220–2229.

Pope III, C.A., Muhlestein, J.B., May, H.T., Renlund, D.G., Anderson, J.L., Horne, B.D., 2006. Ischemic heart disease events triggered by short-term exposure to fine particulate air pollution. Circulation 114 (23), 2443–2448.

Ryou, H.g., Heo, J., Kim, S.-Y., 2018. Source apportionment of PM10 and PM2.5 air pollution, and possible impacts of study characteristics in South Korea. Environ. Pollut. 240, 963–972.

Seinfeld, J.H., Pandis, S.N., 2006. Atmospheric Chemistry and Physics : from Air Pollution to Climate Change, second ed. John Wiley & Sons, Inc.

Seo, J., Park, D.S.R., Kim, J.Y., Youn, D., Lim, Y.B., Kim, Y., 2018. Effects of meteorology and emissions on urban air quality: a quantitative statistical approach to long-term records (1999–2016) in Seoul, South Korea. Atmos. Chem. Phys. 18 (21), 16121–16137.

Shon, Z.H., Kim, K.H., Song, S.K., Jung, K., Kim, N.J., Lee, J.B., 2012. Relationship between water-soluble ions in PM2.5 and their precursor gases in Seoul megacity. Atmos. Environ. 59, 540–550.

Son, J.Y., Lee, J.T., Kim, K.H., Jung, K., Bell, M.L., 2012. Characterization of fine particulate matter and associations between particulate chemical constituents and mortality in Seoul, Korea. Environ. Health Perspect. 120 (6), 872–878.

Stelson, A.W., Friedlander, S.K., Seinfeld, J.H., 1979. A note on the equilibrium relationship between ammonia and nitric acid and particulate ammonium nitrate. Atmos. Environ. 13 (3), 369–371, 1967.

Tian, M., Wang, H., Chen, Y., Zhang, L., Shi, G., Liu, Y., Yu, J., Zhai, C., Wang, J., Yang, F., 2017. Highly time-resolved characterization of water-soluble inorganic ions in PM2.5 in a humid and acidic mega city in Sichuan Basin. China. Sci. Total Environ. 580, 224–234.

Ting, Y.-C., Young, L.-H., Lin, T.-H., Tsay, S.-C., Chang, K.-E., Hsiao, T.-C., 2022. Quantifying the impacts of PM2.5 constituents and relative humidity on visibility impairment in a suburban area of eastern Asia using long-term in-situ measurements. Sci. Total Environ. 818, 151759.

Turner, M.C., Krewski, D., Diver, W.R., Pope III, C.A., Burnett, R.T., Jerrett, M., Marshall, J.D., Gapstur, S.M., 2017. Ambient air pollution and cancer mortality in the cancer prevention study II. Environ. Health Perspect. 125 (8), 087013.

Tutsak, E., Koçak, M., 2019. High time-resolved measurements of water-soluble sulfate, nitrate, and ammonium in PM2.5 and their precursor gases over the Eastern Mediterranean. Sci. Total Environ. 672, 212–226.

Uria-Tellaetxe, I., Carslaw, D.C., 2014. Conditional bivariate probability function for source identification. Environ. Model. Software 59, 1–9.

Wang, G., Zhang, R., Gomez, M.E., Yang, L., Zamora, M.L., Hu, M., Lin, Y., Peng, J., Guo, S., Meng, J., Li, J., Cheng, C., Hu, T., Ren, Y., Wang, Y., Gao, J., Cao, J., An, Z., Zhou, W., Li, G., Wang, J., Tian, P., Oritiz, W., Secrest, J., Du, Z., Zheng, Jing, Shang, D., Zeng, L., Shao, M., Wang, W., Huang, Y., Wang, Y., Zhu, Y., Li, Y., Hu, J., Pan, B., Cai, L., Cheng, Y., Ji, Y., Zhang, F., Rosenfeld, D., Liss, P.S., Duce, R.A., Kolb, C.E., Molina, M.J., 2016. Persistent sulfate formation from London Fog to Chinese haze. Proc. Natl. Acad. Sci. USA 113 (48), 13630–13635.

Wang, Y.L., Song, W., Yang, W., Sun, X.C., Tong, Y.D., Wang, X.M., Liu, C.Q., Bai, Z.P., Liu, X.Y., 2019. Influences of atmospheric pollution on the contributions of major oxidation pathways to PM2. 5 nitrate formation in Beijing. J. Geophys. Res. Atmos. 124 (7), 4174–4185.

Wang, Y., Chen, Y., Wu, Z., Shang, D., Bian, Y., Du, Z., Schmitt, S.H., Su, R., Gkatzelis, G. I., Schlag, P., Hohaus, T., Voliotis, A., Lu, K., Zeng, L., Zhao, C., Alfarra, M.R., McFiggans, G., Wiedensohler, A., Kiendler-Scharr, A., Zhang, Y., Hu, M., 2020. Mutual promotion between aerosol particle liquid water and particulate nitrate enhancement leads to severe nitrate-dominated particulate matter pollution and low visibility. Atmos. Chem. Phys. 20, 2161–2175.

Weber, R., Orsini, D., Daun, Y., Lee, Y.-N., Klotz, P., Brechtel, F., 2001. A particle-into-liquid collector for rapid measurement of aerosol bulk chemical composition. Aerosol Sci. Technol. 35, 718–727.

Won, S.R., Shim, I.-K., Kim, J., Ji, H.A., Lee, Y., Lee, J., Ghim, Y.S., 2021. PM2.5 and trace elements in underground shopping districts in the Seoul metropolitan area, Korea. Int. J. Environ. Res. Publ. Health 18, 297.

Xu, Z., Liu, M., Zhang, M., Song, Y., Wang, S., Zhang, L., Xu, T., Wang, T., Yan, C., Zhou, T., Sun, Y., Pan, Y., Hu, M., Zheng, M., Zhu, T., 2019. High efficiency of livestock ammonia emission controls in alleviating particulate nitrate during a severe winter haze episode in northern China. Atmos. Chem. Phys. 19, 5605–5613.

Zhang, B., Zhou, T., Liu, Y., Yan, C., Li, X., Yu, J., Wang, S., Liu, B., Zheng, M., 2019a. Comparison of water-soluble inorganic ions and trace metals in PM2.5 between online and offline measurements in Beijing during winter. Atmos. Pollut. Res. 10, 1755–1765.

Zhang, H., Li, N., Tang, K., Liao, H., Shi, C., Huang, C., Wang, H., Guo, S., Hu, M., Ge, X., Chen, M., Liu, Z., Yu, H., Hu, J., 2022. Estimation of secondary PM2.5 in China and the United States using a multi-tracer approach. Atmos. Chem. Phys. 22, 5495–5514.

Zhang, X., Zhao, X., Ji, G., Ying, R., Shan, Y., Lin, Y., 2019b. Seasonal variations and source apportionment of water-soluble inorganic ions in PM2.5 in Nanjing, a megacity in southeastern China. J. Atmos. Chem. 76 (1), 73–88.

Zhao, X., Huang, Y., Han, F., Touseef, B., Song, Z., Zhao, X., Bandna, B., 2022. The seasonal characterization and source analysis of water-soluble inorganic ions in PM2.5 in Fuxin, northeast China. Environ. Forensics 1–12.